

# Temperature dependence of birefringence and stress for natural rubber vulcanizates at strained state

Akihiro Suzuki, Hidetoshi Oikawa and Kenkichi Murakami

Chemical Research Institute of Non-Aqueous Solutions, Tohoku University, Sendai 980, Japan

(Received 1 March 1984; revised 24 May 1984)

The temperature dependence of stress and birefringence for natural rubber vulcanizates under medium and large deformation was measured for the processes of cooling, heating and re-cooling. In order to investigate the relation between the stress and crystal phase, the observed birefringence,  $\Delta t$ , was converted into the crystallinity,  $X_v$ , by the following equation:

$$X_v = \frac{\Delta t - \Delta n_a^0 f_a}{\Delta n_c^0 f_c - \Delta n_a^0 f_a}$$

where  $\Delta n_c^0$ ,  $\Delta n_a^0$ ,  $f_a$  and  $f_c$  are the intrinsic birefringence of the crystal, that of the amorphous phase, the orientation factor of crystallites, and that of amorphous phase, respectively. The fusion of crystallites induced by the thermal crystallization resulted in the increasing contractile force, while the fusion of strain-induced crystallites induced the reduction of contractile force.

(Keywords: natural rubber vulcanizates; birefringence; stress; crystallinity; fusion and recrystallization)

## INTRODUCTION

In the previous paper<sup>1</sup> the authors have reported the temperature dependence of birefringence for natural rubber vulcanizates under uniaxial deformation. Since the birefringence varies sensitively for the growth or melting of oriented crystallites, the crystallization and the fusion process for stretched natural rubber vulcanizates could be investigated from the dependence of birefringence on temperature.

In the present article, the stress and the birefringence for specimen at extended state during cooling, heating and re-cooling process were measured simultaneously. The extent of effect of crystallites on the stress for stretched specimen will be discussed.

## EXPERIMENTAL

### Specimens

The material used in this study was natural rubber (Pale crepe No. 1), cured with 4 wt% of dicumene peroxide (DCP). The preparation details and the method of determining crosslink density for specimen were carried out as described elsewhere<sup>1</sup>.

### Measurements and analyses

The apparatus for simultaneously measuring the birefringence and stress is shown in Figure 1. It consists of a stretcher and a chamber in which the temperature is able to vary continuously over the range 223–353 K, and the apparatus is attached to a polarizing microscope.

In Figure 1 the specimen G (25 mm in length, 5 mm in width and 0.5 mm in thickness) is mounted between two stainless steel clamps, E<sub>1</sub> and E<sub>2</sub>. The clamp E<sub>1</sub> is connected to the strain gauge C which is fixed on the

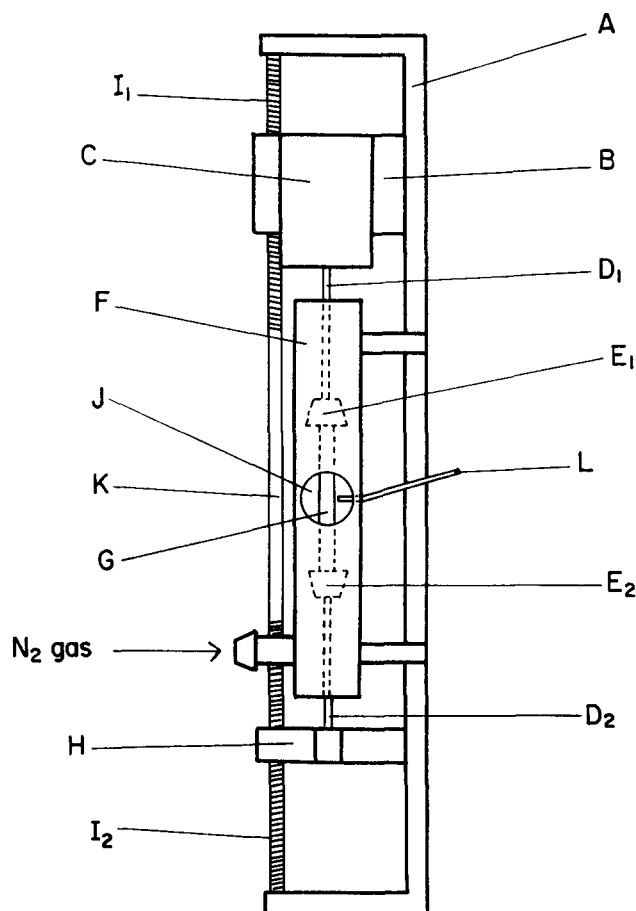
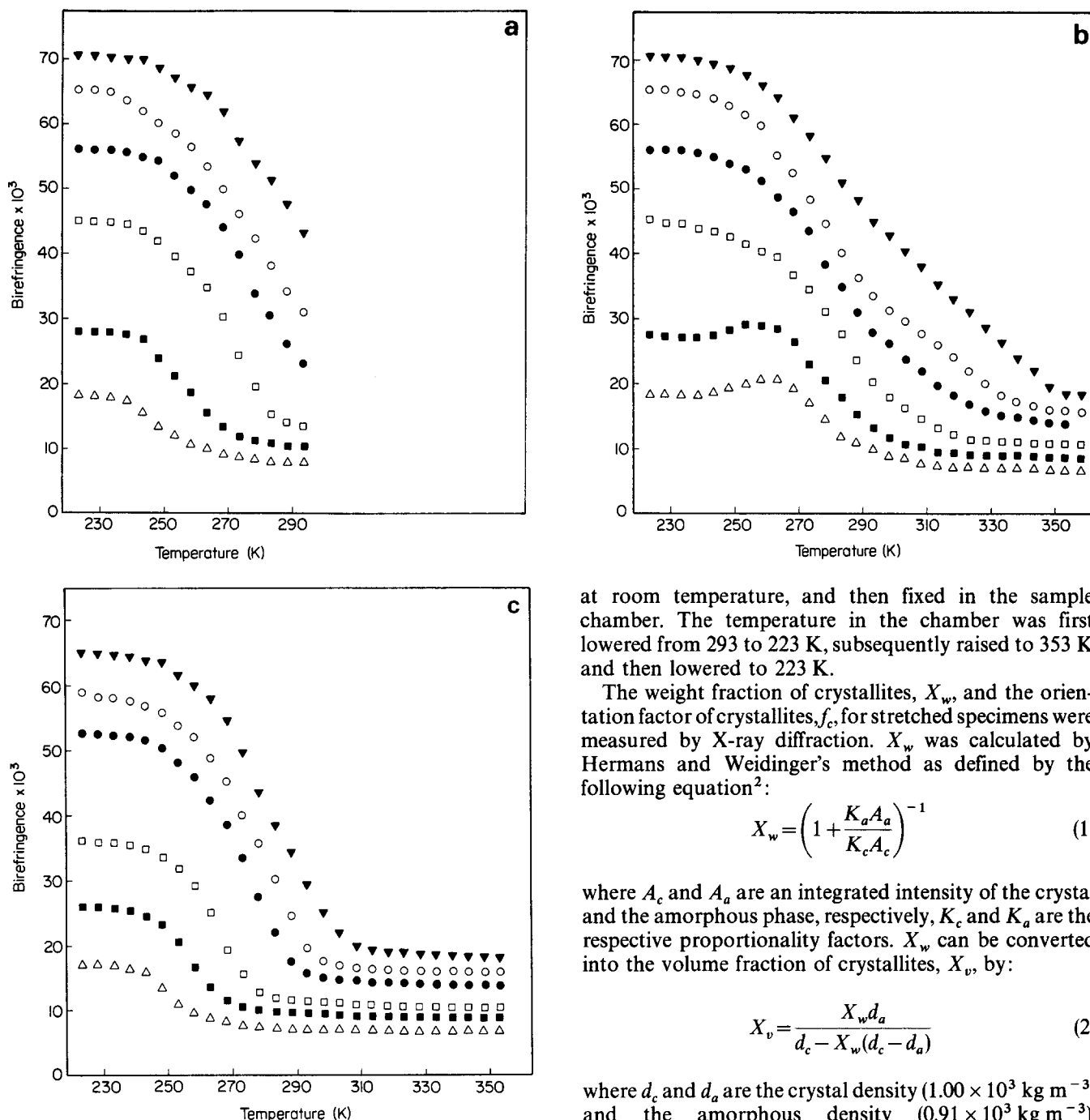


Figure 1 The sketch of the stretcher and the sample chamber. A: flame; B: cross head; C: strain gauge; D<sub>1</sub> and D<sub>2</sub>: fine rod; E<sub>1</sub> and E<sub>2</sub>: clamp; F: sample chamber; G: specimen; H: cross head; I<sub>1</sub>: left-handed screw; I<sub>2</sub>: right-handed screw; J: window of chamber; K: rod with screw; L: thermocouple



**Figure 2** The temperature dependence of birefringence for specimen at various extension ratios. (a) Cooling process; (b) heating process; (c) re-cooling process. ( $\Delta$ ) = 3.0, ( $\blacksquare$ ) = 3.5, ( $\square$ ) = 4.0, ( $\bullet$ ) = 4.5, ( $\circ$ ) = 5.0, ( $\blacktriangledown$ ) = 5.5

crosshead B with a fine stainless steel rod  $D_1$ . The clamp  $E_2$  is joined to crosshead H with the rod  $D_2$ . The crossheads B and H slide smoothly in opposite directions because of a left-handed screw  $I_1$  and a right-handed screw  $I_2$  on both sides of rod K. Thus, the centre of the specimen can be maintained on the window J of sample chamber F at any extension ratio and the birefringence was measured through the window J. The temperature in the chamber is controlled by the changing flow rate of the nitrogen gas cooled in liquid nitrogen or heated in the electric furnace, and is measured by a thermocouple L. The change of temperature in the chamber was at a cooling (or heating) rate of ca.  $0.8\text{--}1.0\text{ K min}^{-1}$ . The specimen was uniaxially deformed at any extension ratio

at room temperature, and then fixed in the sample chamber. The temperature in the chamber was first lowered from 293 to 223 K, subsequently raised to 353 K and then lowered to 223 K.

The weight fraction of crystallites,  $X_w$ , and the orientation factor of crystallites,  $f_c$ , for stretched specimens were measured by X-ray diffraction.  $X_w$  was calculated by Hermans and Weidinger's method as defined by the following equation<sup>2</sup>:

$$X_w = \left(1 + \frac{K_a A_a}{K_c A_c}\right)^{-1} \quad (1)$$

where  $A_c$  and  $A_a$  are an integrated intensity of the crystal and the amorphous phase, respectively,  $K_c$  and  $K_a$  are the respective proportionality factors.  $X_w$  can be converted into the volume fraction of crystallites,  $X_v$ , by:

$$X_v = \frac{X_w d_a}{d_c - X_w(d_c - d_a)} \quad (2)$$

where  $d_c$  and  $d_a$  are the crystal density ( $1.00 \times 10^3\text{ kg m}^{-3}$ ) and the amorphous density ( $0.91 \times 10^3\text{ kg m}^{-3}$ ), respectively<sup>3</sup>.

However,  $f_c$  is defined as the following equation:

$$f_c = \frac{1}{2}(3\langle \cos^2 \phi_{c,z} \rangle - 1) \quad (3)$$

where  $\langle \cos^2 \phi_{c,z} \rangle$  represents the mean-square cosine of the angle between the C axis of the unit cell of the crystallites and the stretching direction, Z axis. The value of  $\langle \cos^2 \phi_{c,z} \rangle$  can be calculated by<sup>4</sup>:

$$\langle \cos^2 \phi_{c,z} \rangle = 1 - 2\langle \cos^2 \phi_{120,z} \rangle \quad (4)$$

where the value of  $\langle \cos^2 \phi_{120,z} \rangle$  was graphically determined from the azimuthal intensity distribution of X-ray diffraction for (120) plane.

## RESULTS AND DISCUSSION

Figure 2 shows the temperature dependence of bire-

fringence during (a) cooling, (b) heating and (c) re-cooling process, respectively. The temperature dependence of birefringence was mentioned in the previous paper<sup>1</sup>.

In order to consider the relation between stress and crystallinity during crystallization or fusion, the change in crystallinity during these processes was obtained from the temperature dependence of birefringence by the procedure described below.

In general, the observed birefringence,  $\Delta t$ , for crystalline polymers mainly consists of the sum of the birefringence of the crystal phase,  $\Delta t_c$ , and the amorphous phase,  $\Delta t_a$ , which are given by:

$$\Delta t_c = \Delta n_c^\circ f_c X_v \quad (5)$$

$$\Delta t_a = \Delta n_a^\circ f_a (1 - X_v) \quad (6)$$

where  $\Delta n_c^\circ$ ,  $\Delta n_a^\circ$  and  $f_a$  are the intrinsic birefringence for crystal phase, that for amorphous phase and the orientation factor of amorphous phase, respectively.

Thus,  $\Delta t$  is expressed by<sup>5</sup>:

$$\Delta t = \Delta t_c + \Delta t_a + \Delta F = \Delta n_c^\circ f_c X_v + \Delta n_a^\circ f_a (1 - X_v) + \Delta F \quad (7)$$

where  $\Delta F$  indicates the form birefringence. The value of  $\Delta F$  is usually so small, compared with the other terms, that the third term can be neglected in equation (7).

Therefore, one can obtain:

$$\Delta t = \Delta t_c + \Delta t_a = \Delta n_c^\circ f_c X_v + \Delta n_a^\circ f_a (1 - X_v) \quad (8)$$

In order to estimate  $X_v$  from  $\Delta t$ , equation (8) can be rewritten as follows:

$$X_v = \frac{\Delta t - \Delta n_a^\circ f_a}{\Delta n_c^\circ f_c - \Delta n_a^\circ f_a} \quad (9)$$

The values for  $\Delta n_c^\circ$  and  $\Delta n_a^\circ f_a$  need to be evaluated  $X_v$  from equation (9).

The values of  $\Delta n_a^\circ f_a$  were determined experimentally by the method reported in the previous paper<sup>1</sup>, and are shown in Table 1.

Equation (8) can be rewritten in order to estimate the value of  $\Delta n_c^\circ$ :

$$\frac{\Delta t - \Delta t_a}{f_c} = \frac{\Delta t_c}{f_c} = \Delta n_c^\circ X_v \quad (10)$$

Figure 3 indicates the plots of  $\Delta t_c/f_c$  vs.  $X_v$ . The values of  $f_c$  and  $X_v$  used were determined by X-ray diffraction, respectively, and are given in Table 2. The value of  $\Delta n_c^\circ$  determined from the slope of the straight line in Figure 3 was 0.140, and agrees well with the theoretical value (0.163)<sup>6</sup> within experimental error.

**Table 1** The birefringence contributions of the pure amorphous phase at various extension ratio

$\alpha$	$\Delta n_a^\circ f_a \times 10^3$
4.0	10.8
4.5	14.5
5.0	15.9
5.5	18.5

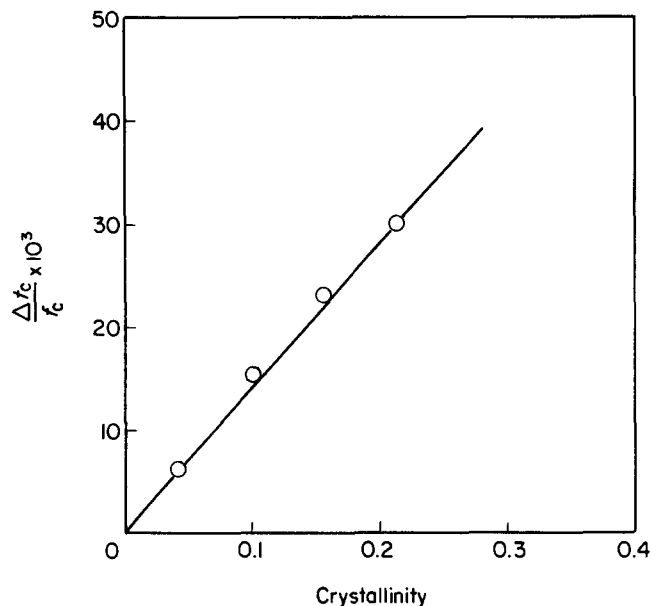


**Figure 3** Changes of birefringence attributed to oriented crystallinity estimated by X-ray diffraction

**Table 2** The crystallinity and the orientation factor of crystallites determined from X-ray diffraction

$\alpha$	$X_v^*$	$f_c$
4.0	0.038	0.979
4.5	0.096	0.980
5.0	0.154	0.983
5.5	0.212	0.985

\*The values of  $X_w$  were converted into  $X_v$  by equation (2)

**Table 3** The apparent melting temperature,  $T_m$ , at various extension ratio

$\alpha$	$T_m$ (K)
3.0	298
3.5	303
4.0	319
4.5	328
5.0	339
5.5	350

Consequently, the conversion of  $\Delta t$  into  $X_v$  can be carried out by using the following equation:

$$X_v = \frac{\Delta t - \Delta n_a^\circ f_a}{0.14 f_c - \Delta n_a^\circ f_a} \quad (11)$$

The change of  $f_c$  with temperature was so small that the values of  $f_c$  could be regarded as constant.

Figure 4 shows the temperature dependence of crystallinity,  $X_v$ , estimated by equation (11) for specimens at extension ratios > 4.0 on cooling, heating and re-cooling. The crystal growth proceeded rapidly during cooling.  $X_v$  became constant in the range of temperature below 230 K, and the values of  $X_v$  was significantly dependent on the extension ratio,  $\alpha$  (Figure 4a).

As shown in Figure 4b, the decreasing of  $X_v$  on heating

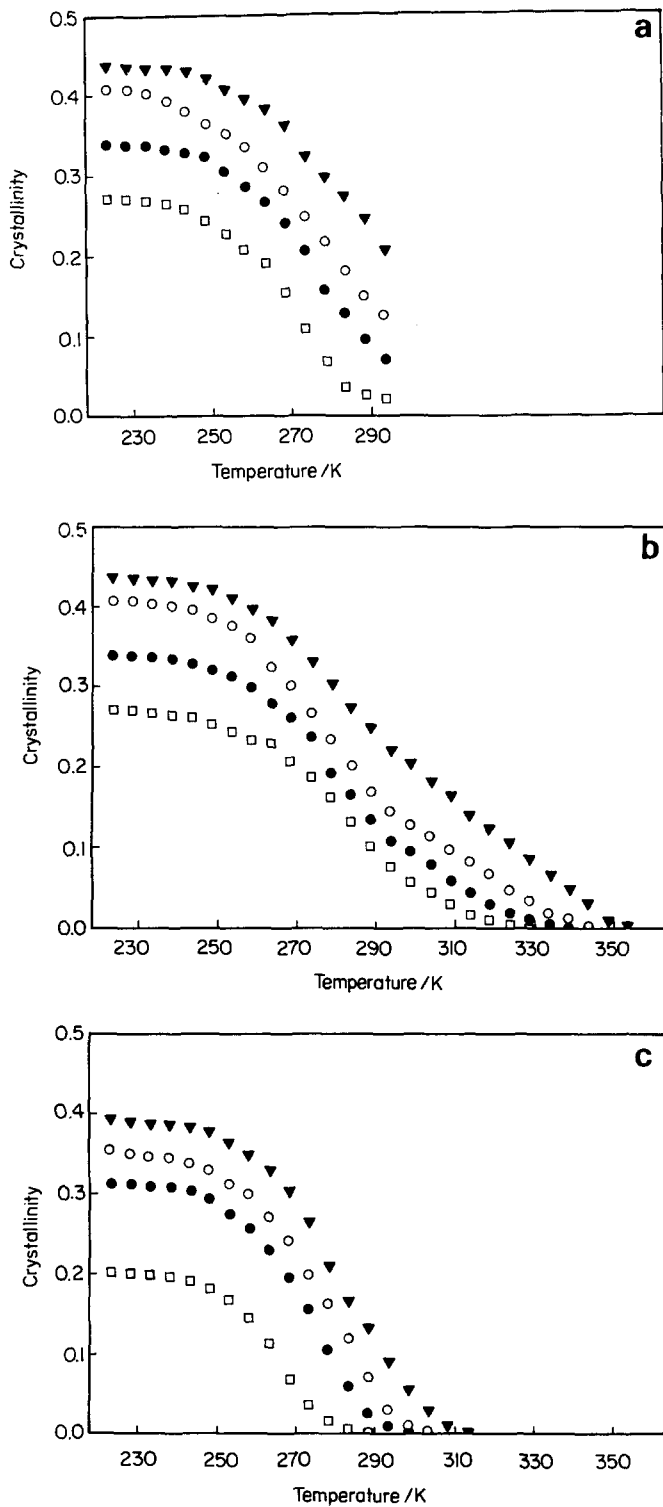


**Figure 4** The temperature dependence of crystallinity estimated by equation (11) for specimens at extension ratio of  $> 4.0$ . (a) Cooling process; (b) heating process; (c) re-cooling process. Symbols as in Figure 2

indicates the fusion of the crystallites. The apparent melting point,  $T_m$ , which was defined at  $X_v = 0$  rose with  $\alpha$ , and then are given in Table 3.

The values of  $X_v$  on re-cooling process began to increase in the temperature range 290–310 K at any  $\alpha$ , and the growth of crystal proceeded with decreasing temperature<sup>7</sup>.

Figure 5 shows the temperature dependence of stress for strained specimen. The stress on cooling as shown in

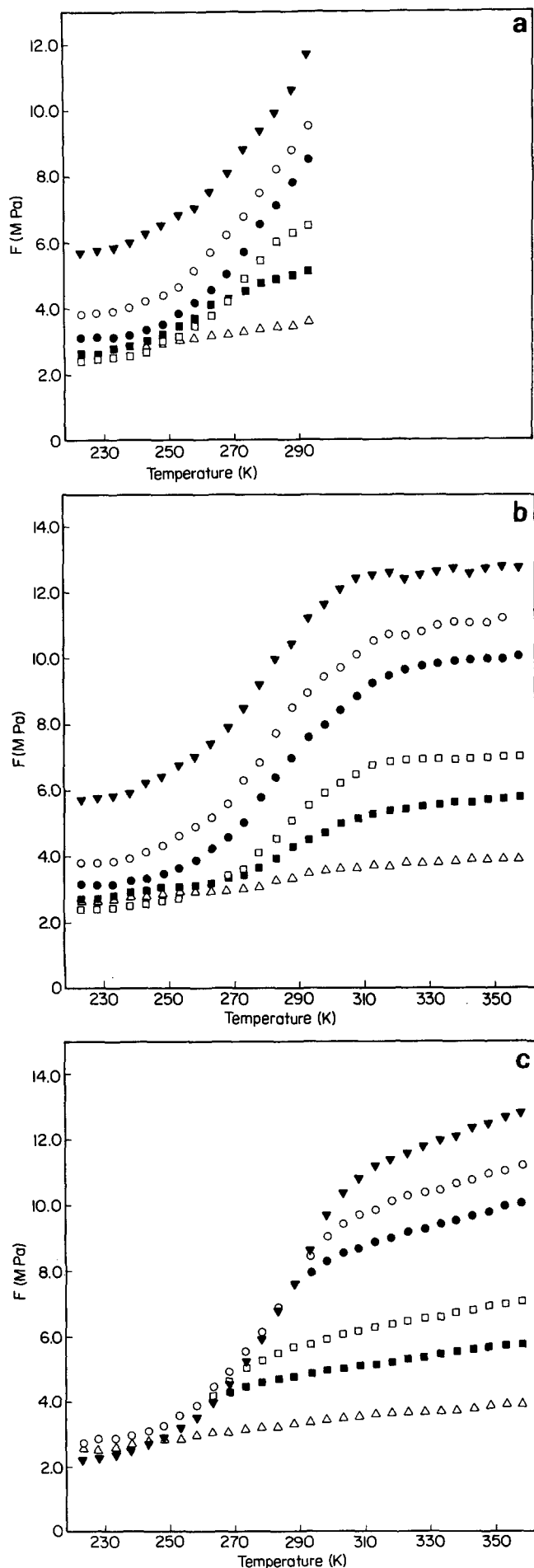


**Figure 5** The temperature dependence of stress for specimen at various extension ratios. (a) Cooling process; (b) heating process; (c) re-cooling process. Symbols as in Figure 2

Figure 5a decreased gradually with decreasing temperature. In particular, the degree of stress decrease under large deformation ( $\alpha=5.0$  and  $\alpha=5.5$ ) was much larger than that under medium deformation ( $\alpha=4.0$  and  $\alpha=4.5$ ). The reduction of stress during cooling is primarily attributed to the decreasing number of network chains in the amorphous phase with the development of the crystal, rather than the reduction of the thermo-mobility of amorphous network chains at low temperature.

On the heating (Figure 5b) the stress increased rapidly in the temperature range 240–310 K because of the partial melting of the crystallites, and enhanced slightly at temperatures  $> 310$  K, which approximately corresponds to  $T_m$ .

The stress for specimens at fixed strain during subsequent re-cooling diminished in the temperature range 300–250 K as shown in Figure 4c.

Figure 6 indicates the relation between  $F/T$  and  $X_v$

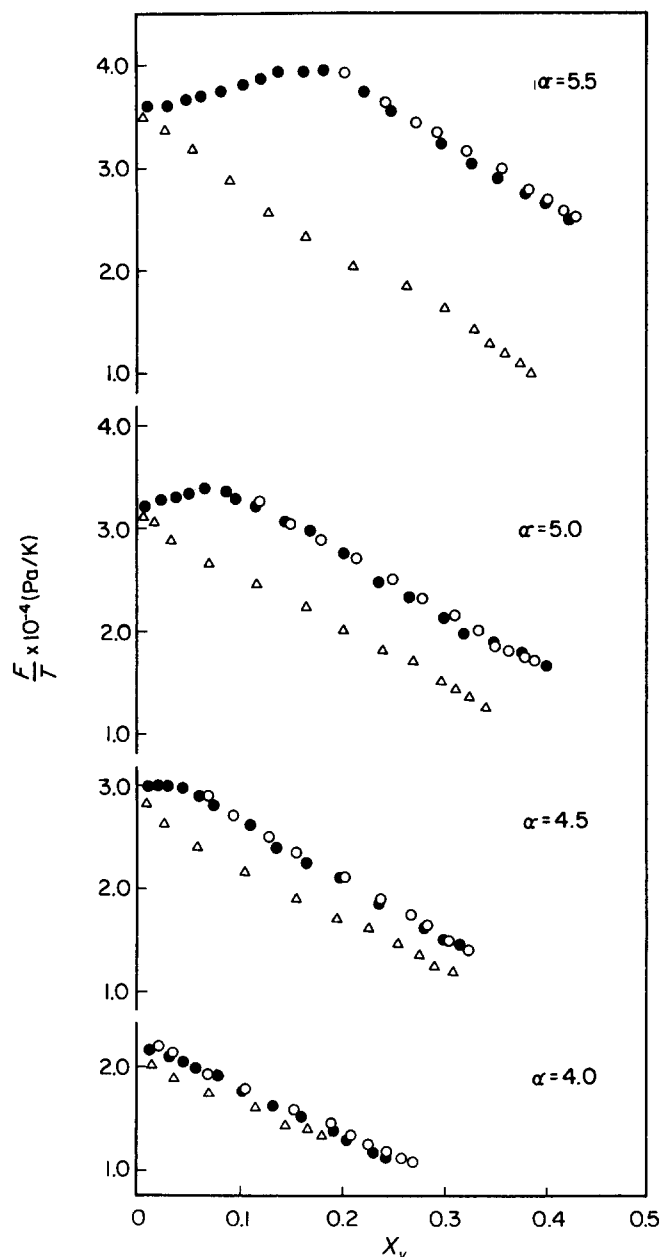


Figure 6 Variations in stress divided by absolute temperature with crystallinity for each process. (○) Cooling process over the temperature range 293–223 K; (●) heating process over the temperature range 223–353 K; (△) re-cooling process over the temperature range 353–223 K

during cooling, heating and re-cooling. The plot of  $F/T$  against  $X_v$  at  $\alpha=4.0$  was linear in all cases. However, the plot of  $F/T$  vs.  $X_v$  at extension ratio of more than 4.5 was different from that at  $\alpha=4.0$ . That is the values of  $F/T$  decreased linearly on the cooling process. On the other hand, after the values of  $F/T$  increased on the same path as the cooling process, they decreased gradually through the maximum value at a certain  $X_v$  during subsequent heating. Further, on re-cooling the value of  $F/T$  diminished linearly with increasing  $X_v$  (or decreasing temperature) on a different path from the heating process.

The melting process of crystallites in the network under large deformation was divided into two steps from the degree of  $F/T$ : (1) the fusion process (I) due to partial melting of the crystal phase, corresponds to increasing  $F/T$  with decreasing  $X_v$ ; (2) the fusion process (II) based upon the disappearance of the crystallites as crosslink points, corresponds to the decreasing  $F/T$  with  $X_v$ .

On the basis of the above experimental results described, the dependence of the relation between the stress and network structure, under large deformation, on temperature may be explained by using the model illustrated in Figure 7 as mentioned below.

It is well known that the crystallites are formed in the network when natural rubber vulcanizate is stretched at room temperature, and the crystallites can be regarded as crosslink points. Consequently, the network structure under large deformation is composed of the chemical crosslink points and secondary crosslinkages such as the strain-induced crystallites and the intermolecular entanglements as shown in Figure 7b. When the stretched natural rubber vulcanizate is cooled, the crystallites may grow further along the deformation direction than along the lateral direction (Figure 7c)<sup>8</sup>. The contractile force reduced gradually with development of the crystal due to the decreasing of the amorphous network chains<sup>9</sup>.

On subsequent fusion, the crystallites partially melt, the contractile force then increases<sup>10</sup> until the crystallites which act as crosslink points exist in the stretched network (Figure 7d).

The strain-induced crystallites at room temperature begin to melt at temperatures  $> 300$  K, which induces intermolecular slipping and results in the reduction of the contractile force (Figure 7e).

After complete melting of the crystal phase, the contractile force reduces and the crystals again develop on re-cooling (Figure 7f).

## CONCLUSION

The crystallinity of natural rubber vulcanizates under deformation can be calculated from the temperature dependence of birefringence.

Intrinsic birefringence for the crystal phase,  $\Delta n_c^\circ$ , was obtained experimentally from X-ray diffraction and the temperature dependence of birefringence, and the value of  $\Delta n_c^\circ$  was 0.140. The experimental value was in fair agreement with the theoretical value (0.163).

The stretched natural rubber vulcanizates at lower temperature included the crystallites which developed by both strain-induced and thermal crystallization. The melting of the crystal phase induced by thermal crystallization caused  $F/T$  to increase, while the fusion of the strain-induced crystallites resulted in reduction of  $F/T$ .

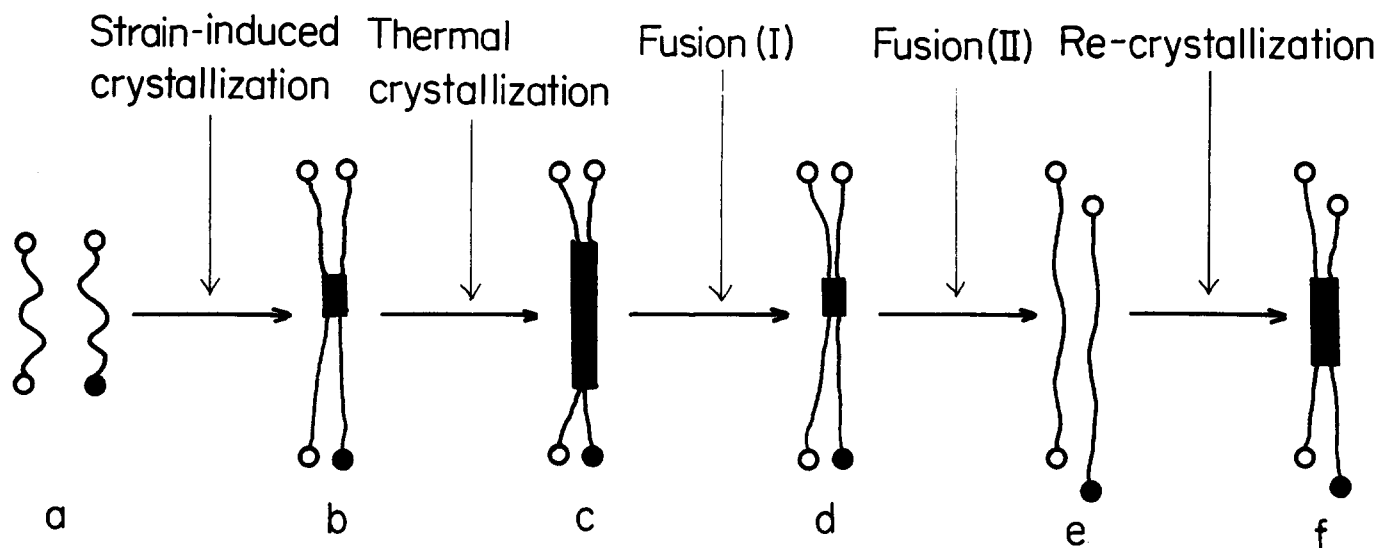


Figure 7 The crystallization and the fusion for stretched specimen during cooling, heating and re-cooling. (○) Chemical crosslink point; (●) intermolecular entanglement; (■) crystal phase

#### REFERENCES

- |  |   |
|--|---|
| <p>1 Suzuki, A., Oikawa, H. and Murakami, K. <i>Polymer</i> 1985, <b>26</b>, 97</p> <p>2 Weidinger, A. and Hermans, P. H. <i>Makromol. Chem.</i> 1961, <b>50</b>, 98</p> <p>3 Keller, A. 'Growth and Perfection of Crystals' (Ed. D. Turnbull), John Wiley and Son, New York, 1958</p> <p>4 Wilchinsky, Z. W. <i>J. Appl. Phys.</i> 1959, <b>30</b>, 792</p> | <p>5 Stein, R. S. and Norris, F. H. <i>J. Polym. Sci.</i> 1956, <b>21</b>, 381</p> <p>6 Bunn, C. W. 'Chemical Crystallography', Oxford Clarendon Press, 1961</p> <p>7 Oth, J. F. and Flory, P. J. <i>J. Am. Chem. Soc.</i> 1958, <b>80</b>, 1297</p> <p>8 Gent, A. N. <i>Trans. Faraday Soc.</i> 1954, <b>50</b>, 521</p> <p>9 Smith Jr., K., Greene, A. and Ciferri, A. <i>Kolloid-Z. Z. Polym.</i> 1964, <b>194</b>, 49</p> <p>10 Flory, P. J. <i>J. Am. Chem. Soc.</i> 1956, <b>78</b>, 5222</p> |
|--|---|